PONTIFICIA UNIVERSIDAD CATÓLICA DEL PERÚ

ESCUELA DE POSGRADO

Mutual Unbiasedness in Coarse-Grained Continuous Variables

Artículo para optar el grado de Magíster en Física que presenta:

Autor:
Piero Leopoldo Sánchez Melgar

Asesores:
Prof. Francisco de Zela
Prof. Daniel S. Tasca

Jurado:
Prof. Francisco de Zela
Prof. Daniel S. Tasca
Prof. Eduardo Massoni

Lima, 2018

Resumen

En este trabajo se investiga la noción de imparcialidad mutua para mediciones de grano grueso en sistemas cuánticos con variables continuas. Se muestra que mientras que el procedimiento estándar de granulación gruesa rompe la imparcialidad mutua entre variables conjugadas, dicha imparcialidad puede, en cambio, establecerse teóricamente y observarse experimentalmente con granulación gruesa periódica. Se exhiben los resultados predichos mediante un experimento óptico que implementa la difracción de Fraunhofer a través de una red de difracción periódica, encontrándose excelente acuerdo con la teoría. Nuestros resultados representan un avance importante en el desarrollo de una conexión formal entre la mecánica cuántica de variable discreta y la de variable continua.
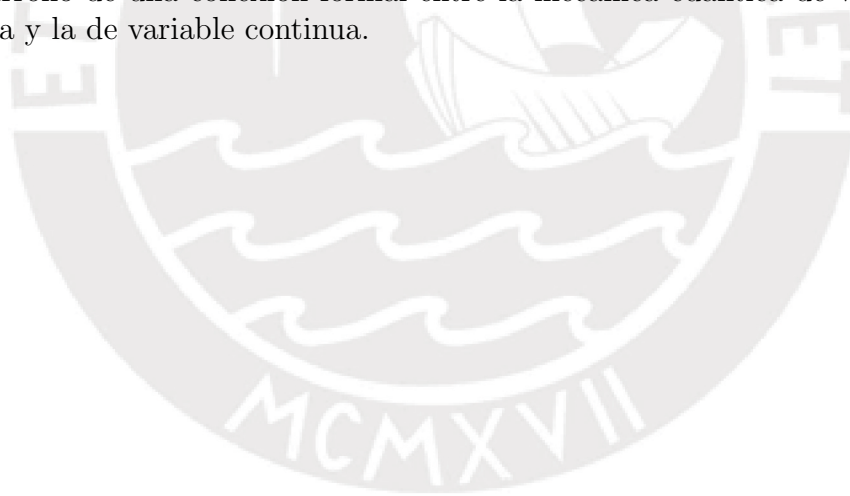
Agradecimientos

Sin lugar a dudas, este trabajo no sería posible sin la ayuda y el apoyo de una gran cantidad de personas a las cuales quiero agradecer.

Gracias a mi familia por darme la seguridad y el soporte necesarios para que avance en mi carrera. Especialmente a mi madre, quien desde pequeño me ha enseñado a siempre dar lo mejor de mí. Agradezco también a Victor Canessa por brindarme su compañía y la confianza que necesitaba en los momentos en que más dudé de mí mismo.

Gracias a mis amigos y compañeros por hacer el viaje más divertido y permitirme aprender de ellos. A todos los miembros del laboratorio de Óptica Cuántica de la Pontificia Universidad Católica del Perú les debo mucho por toda su experiencia y ayuda en diversos proyectos.

Gracias al profesor Francisco de Zela por sus enseñanzas y todo el apoyo que me ha dado. Especialmente por la oportunidad de viajar a Brasil donde principalmente desarrollé este proyecto. Aprovecho también en agradecer al profesor Antonio Z. Khoury por permitirme trabajar en su laboratorio en la Universidad Federal Fluminense, así como al profesor Daniel S. Tasca quien estuvo a cargo del experimento del cual formé parte y que presento en esta tesis.

Finalmente, agradezco a CIENCIACTIVA-CONCYTEC por darme la beca que me permitió estudiar esta maestría.

Mutual Unbiasedness in Coarse-grained Continuous Variables

Daniel S. Tasca,[1, *] Piero Sánchez,[2] Stephen P. Walborn,[3] and Łukasz Rudnicki[4, 5, †]

[1]*Instituto de Física, Universidade Federal Fluminense, Niterói, RJ 24210-346, Brazil*
[2]*Departamento de Ciencias, Sección Física, Pontificia Universidad Católica del Perú, Apartado 1761, Lima, Peru*
[3]*Instituto de Física, Universidade Federal do Rio de Janeiro,*
Caixa Postal 68528, Rio de Janeiro, RJ 21941-972, Brazil
[4]*Max-Planck-Institut für die Physik des Lichts, Staudtstraße 2, 91058 Erlangen, Germany*
[5]*Center for Theoretical Physics, Polish Academy of Sciences, Al. Lotników 32/46, 02-668 Warsaw, Poland*

The notion of mutual unbiasedness for coarse-grained measurements of quantum continuous variable systems is considered. It is shown that while the procedure of "standard" coarse graining breaks the mutual unbiasedness between conjugate variables, this desired feature can be theoretically established and experimentally observed in periodic coarse graining. We illustrate our results in an optics experiment implementing Fraunhofer diffraction through a periodic diffraction grating, finding excellent agreement with the derived theory. Our results are an important step in developing a formal connection between discrete and continuous variable quantum mechanics.

Introduction. The ability to measure a system in an infinite number of non-commuting bases distinguishes the quantum world from classical physics. Wave-particle duality and more generally the complementarity principle are directly rooted in this feature of quantum mechanics. Though one can measure a quantum system in several distinct bases, uncertainty relations limit the amount of information that can be obtained. It is well known that projection onto an eigenstate of one basis reduces the information that can be obtained through or inferred about subsequent measurement in a different basis. The information is minimum for mutually unbiased bases (MUBs) [1, 2], for which all outcomes of the second measurement are equally likely, so that total uncertainty is always substantial (the sharpest uncertainty relations [3]) and most insensitive to input states [4]. MUBs play an important role in complementarity [5], quantum cryptography [6] and quantum tomography [7, 8], are useful for certifying quantum randomness [9], and for detecting quantum correlations such as entanglement [10–12] and steering [13–20].

Quantum information encoding in high-dimensional systems harbor the potential for efficient quantum cryptography [21–23] and interesting fundamental studies [24, 25]. A number of modern day implementations of high-dimensional quantum systems rely on continuous variables (CV) encoded in photonics systems. These CV [26] or hybrid [27] platforms allow one to encode several bits per outcome. However, a typical measurement device does not register a continuous and infinite range of values, and it is thus necessary to consider discretized measurements. A most common approach is the selection of a finite set of transverse spatial modes labeled by discrete mode indexes [28–31], for which MUB measurements are attainable by the use of phase holograms [8]. Free-space [32], multicore fibers [33] or on-chip [34] path encoding as well as time-bin [35] are also interesting techniques with potencial for high-dimensionality. These methods, despite being useful, discard a fraction of available modes and do not straightforwardly extend to the complementary (Fourier) domain of CVs. A different discretization procedure is the *coarse graining* of the continuous degree of freedom itself [36, 37]. In this case, practical constraints such as finite detector resolution, or limited measurement time and sampling range, if not properly handled, can lead to false conclusions in tasks such as entanglement detection and cryptographic security [15, 38, 39].

The notion of quantum mechanical mutual unbiasedness seems rather well established. In particular, two orthonormal bases $|a_i\rangle$ and $|b_j\rangle$, $i, j = 0, \ldots, d - 1$, in a finite-dimensional Hilbert space (of dimension d) are mutually unbiased if and only if $|\langle a_i | b_j \rangle| = 1/\sqrt{d}$ for all i, j (MUB condition) [40]. This definition (for finite d) can be extended to deal with—so-called—mutually unbiased (nonprojective [62]) measurements [41]. For continuous variables, such as a conjugate pair formed by position and momentum, mutual unbiasedness is encoded in the relation $|\langle x | p \rangle| = 1/\sqrt{2\pi\hbar}$ [42]. One might suspect that coarse graining preserves the original unbiasedness of continuous variables. We shall explain below why this is not the case for standard coarse graining, and further construct a set of coarse-grained mutually unbiased measurements of finite cardinality. The latter property may in principle allow for a conceptual relationship between CV and finite dimensional quantum mechanics. We demonstrate our results in an optics experiment exploring the transverse position and momentum of a paraxial light field as conjugate CVs. The proposed coarse graining is implemented and mutual unbiasedness is observed for measurement dimensionality up to $d = 15$. Our coarse-graining model, in contrast to most of the discretization methods mentioned above, does not rely on the selection of a *subspace* of all available modes and delivers the MUBs in complementary domains. Thus, mutual unbiasedness in high-dimensional measurements is achieved without the assumption that operations [43, 44] will not transfer the photon state out of the relevant subspace.

Unbiased coarse-grained measurements. In the most basic scenario, one can describe experimental outcomes of coarse-grained position-momentum measurements by means of the projectors [15, 16, 36, 37] ($k, l \in \mathbb{Z}$):

$$A_k = \int_{k_-\Delta}^{k_+\Delta} dx \, |x\rangle \langle x|, \quad B_l = \int_{l_-\delta}^{l_+\delta} dp \, |p\rangle \langle p|, \tag{1}$$
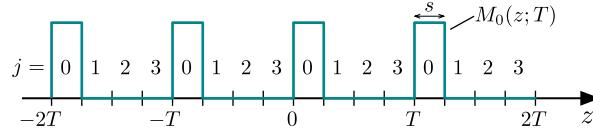
Figure 1: Periodic coarse-graining scheme for $d \equiv T/s = 4$. A diagram of the mask function (4) for $j = 0$ is also represented.

with $j_\pm = j \pm 1/2$. The two parameters Δ and δ are the coarse-graining widths, which can be understood as resolutions of the detectors used in an experiment. Looking at the explicit representations it is quite easy to deduce that $\mathrm{Tr}\,(A_k B_l) = \Delta\delta/2\pi\hbar$. The fact that the overlap does not depend on indices k and l suggests that the operators in Eq. (1) are interrelated in a special way—so-called Accardi complementarity [45]. Note, however, that the constant-trace condition alone is not even enough to assure that original variables are connected by the Fourier transformation [46]. On the other hand, a quantum state localized in one coarse-grained basis, for instance $\psi(x) = 1/\sqrt{\Delta}$ for $|x| \le \Delta/2$ (and 0 elsewhere) that is covered by A_0, *is not* evenly spread with respect to the second one (here given by $\{B_l\}$) but instead decays like the sinc function.

In the last observation, we actually pointed out that the pair of projective measurements (1) does not meet the most natural definition of mutual unbiasedness in discrete settings that can be formulated as follows. Given a pure state $|\Psi\rangle$ and two sets of $d > 1$ projective measurements, $\{\Pi_k\}$ and $\{\Omega_l\}$, we define the usual probabilities $q_k(\Psi) = \langle\Psi|\,\Pi_k\,|\Psi\rangle$ and $p_l(\Psi) = \langle\Psi|\,\Omega_l\,|\Psi\rangle$. The measurements are mutually unbiased if for all $|\Psi\rangle$ and all $k_0, l_0 = 0, \dots, d-1$:

$$q_k(\Psi) = \delta_{k_0 k} \implies p_l(\Psi) = d^{-1}, \tag{2a}$$

$$p_l(\Psi) = \delta_{l_0 l} \implies q_k(\Psi) = d^{-1}. \tag{2b}$$

Again in words, whenever the state is localized in one set, it is evenly spread in the second one. The case with countably infinite sets of projectors [like those in Eq. (1), which however do not fit into the definition] shall be understood in the limit $d \to \infty$. Extension to genuinely continuous scenario would require subtle modifications of the definition; this case is however beyond our interest here. Whenever the pairs of projective measurements are unitarily equivalent, a single requirement is sufficient. Quite obviously, this definition correctly reproduces the MUB condition.

As standard coarse graining (1) does not satisfy the definition (2), we consider now another type of coarse graining. In general, one can define projectors

$$\Pi_k = \int_{\mathbb{R}} dx\, M_k\,(x - x_{\mathrm{cen}}; T_x)\,|x\rangle\,\langle x|, \tag{3a}$$

$$\Omega_l = \int_{\mathbb{R}} dp\, M_l\,(p - p_{\mathrm{cen}}; T_p)\,|p\rangle\,\langle p|, \tag{3b}$$

where M is a "mask function" modelling the detector aperture, T_x and T_p play the role of coarse-graining widths, and we allow extra displacement parameters x_{cen} and p_{cen} representing positioning degrees of freedom setting the masks' origins. We now define d-dimensional periodic coarse graining (PCG) by considering the mask functions ($j = 0, \dots, d-1$)

$$M_j(z; T) = \begin{cases} 1, & j\,s \le z\,(\mathrm{mod}\,T) < (j+1)s \\ 0, & \text{otherwise} \end{cases}, \tag{4}$$

as periodic square waves with spatial period T and bin width $s = T/d$, as illustrated in Fig. 1. The periodic functions (4) define $d > 1$ orthogonal regions covering the whole CV domain: $\sum_{k=0}^{d-1}\Pi_k = \mathbb{I} = \sum_{l=0}^{d-1}\Omega_l$. This model of coarse graining thus assigns a discrete (and finite) measurement outcome "j" to the detection of the quantum particle's CV degree of freedom "z" within the region defined by the mask function $M_j(z; T)$. In Ref. [47], a variant of the periodic masks (4) was used as analyser to test for spatial entanglement of photon pairs.

We are ready to establish the main theoretical result. If [63]

$$\frac{T_x T_p}{2\pi\hbar} = \frac{d}{m}, \quad m \in \mathbb{N} \quad \text{s.t.} \quad \forall_{n=1,\dots,d-1}\; \frac{m\,n}{d} \notin \mathbb{N}, \tag{5}$$

then the projective measurements (3) with the mask function (4) fulfill Eq. (2), thus being mutually unbiased. Since for $m_0 d \le m \le (m_0 + 1)d$ with $m_0 \in \mathbb{N}$ one finds $mn/d = m_0 n + [m\,(\mathrm{mod}\,\mathrm{d})]\,n/d$, the last condition in Eq. (5) is in
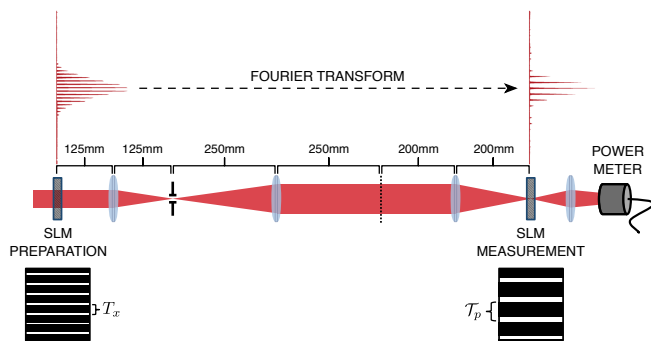
Figure 2: Sketch of the experimental setup used for the demonstration of unbiased coarse-grained measurements. The transverse field distribution of a laser beam is prepared and measured using periodic spatial masks displayed on SLMs. Preparation and measurement sites are connected via optical Fourier transform. The light power transmitted through preparation and measurement spatial masks is monitored with an optical power meter.

general concerned with $m' := m \pmod{d}$. Of special significance is the case $m' = 1$, since the discussed condition is valid for all dimensions. On the other hand, $m' = 0$ is always excluded, which fully corresponds to the fact that for $m = m_0 d$ the left part of Eq. (5) describes communing periodic sets [48–50], i.e. $[\Pi_k, \Omega_l] = 0$, for all k, l. In this particular case there is neither room for unbiasedness nor complementarity.

To gain more intuition we observe that, for instance, if $d = 7$ then all values of $0 < m' < d$ are allowed since 7 is a prime number, while for $d = 10$ only $m' = 1, 3, 7, 9$ fulfill the right condition (note that $n = 4, 6, 8$ all rule out $m' = 5$). For $d = 9$, we obtain $m' = 1, 2, 4, 5, 7, 8$, while for $d = 8$ we get $m' = 1, 3, 5, 7$. Let us finally mention that x_{cen} and p_{cen} play no role for unbiasedness. Before proceeding further, note that first part of Eq. (5) can also be put in equivalent forms: (a) $s_x s_p = 2\pi/md$, (b) $T_x s_p = 2\pi/m$ or (c) $s_x T_p = 2\pi/m$.

To show Eq. (2a), we represent [51] the probability associated with Ω_l in terms of the position autocorrelation function [52]:

$$p_l(\Psi) = \frac{1}{d} + \sum_{N \in \mathbb{Z}/\{0\}} \frac{1 - e^{-(2\pi i N/d)}}{2\pi i N} e^{iN\varphi_l} \int_{\mathbb{R}} dx\, \psi^*(x) \psi(x + N\tau_p), \tag{6}$$

with $\psi(x) = \langle x | \Psi \rangle$, $\varphi_l = -2\pi l/d - p_{\text{cen}}\tau_p/\hbar$ and $\tau_p = 2\pi\hbar/T_p$. Assume first that $q_k(\Psi) = \delta_{k_0 k}$ for an arbitrary k_0. This means that $\psi(x)$ is localized within a single periodic mask, so that the autocorrelation term, which due to Eq. (5) equals $\psi^*(x)\psi(x + mNT_x/d)$, does not vanish only when mN/d is an integer. Due to the further requirement, however, $mN/d \in \mathbb{Z}$ if and only if $N/d \in \mathbb{Z}$. But in this special case the factor $1 - e^{-(2\pi i N/d)}$ becomes equal to 0, so that all terms in the sum in Eq. (6) do vanish, leaving the bare contribution $1/d$. The same type of derivation applies to Eq. (2b). To conclude, the set defined in Eq. (3) is mutually unbiased in a finite-dimensional manner, even though traces of all products $\Pi_k\Omega_l$ are clearly infinite.

Experimental Setup. The formal analogy between paraxial optics and non-relativistic quantum mechanics [53] allows us to experimentally verify the condition of mutual unbiasedness (5) using a simple optical setup implementing Fraunhofer diffraction through a multiple slit aperture. As sketched in Fig. 2, a paraxial HeNe laser beam diffracts from preparation to measurement sites placed at the front and back focal planes of a Fourier transform lens system, respectively. At both sites, we use a spatial light modulator (SLM) to display amplitude spatial masks modelled according to our periodic coarse graining (4) along the vertical direction. The illumination of the preparation SLM by the collimated laser beam with Gaussian transverse profile generates a periodically modulated beam whose intensity distribution at the measurement SLM is that of an interference pattern produced by a periodic diffraction grating, as illustrated in Fig. 2. The intensity distribution of this diffracted beam is then analyzed by periodic spatial masks displayed on the measurement SLM [64].

In our experiment, the conjugate CV stand for the transverse position (x) and momentum (p) of the paraxial light field. As the transverse spatial variables at preparation and measurement sites are related via Fourier transform, the positions at the measurement SLM correspond to the transverse momentum component at the preparation SLM. Denoting $\mathcal{T}_p$ as the physical periodicity (units of length) of the spatial masks applied to the measurement SLM, we translate it to momentum domain as $T_p = \mathcal{T}_p/\alpha$, where the constant $\alpha = f_e \lambda/(2\pi)$ relates to the optical Fourier transform (we set $\hbar = 1$): $f_e = 100$mm is the effective focal length; $\lambda = 633$nm is the light field wavelength. In terms of the physical periodicities and experimental parameters, condition (5) reads $T_x \mathcal{T}_p = f_e \lambda d/m$.

Results. Let us denote by $|\Psi_k\rangle = \mathcal{N}_k^{-1}\Pi_k|\Psi\rangle$ the projections of the state onto the k-th mask ($\mathcal{N}_k$ is a normalization constant), which by construction are eigenstates of Π_k. We perform the experiment with the building function $\psi(x) \equiv \langle x | \Psi \rangle$ a
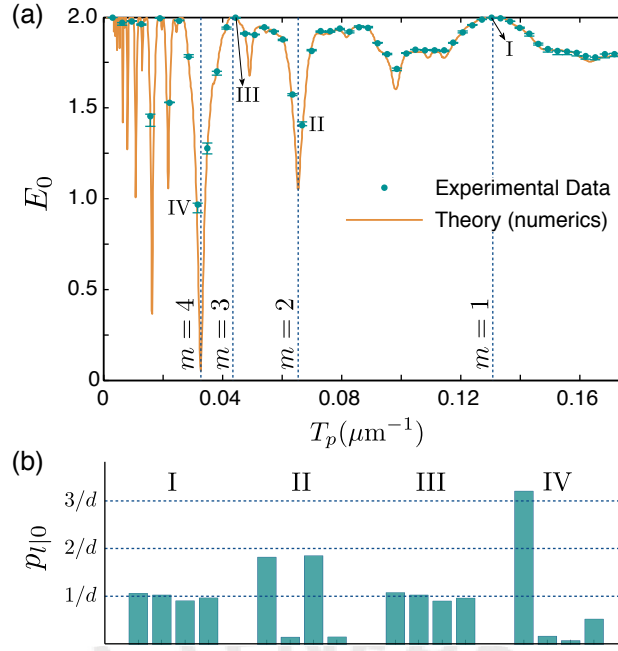
Figure 3: (a) Entropy plot associated with outcomes' probabilities of PCG measurements with $d = 4$ and $T_x = 192\mu$m, as a function of T_p. (b) Examples of measured outcome distributions $p_{l|0}$ for the selected data points shown in plot (a). Unbiasedness ($p_{l|0} \approx 1/d$) is shown for data points I and III.

Gaussian given by the transverse profile of the laser beam at the preparation SLM: $\psi(x) \propto \exp(-x^2/(4\sigma^2))$, with $\sigma = 520\mu$m.

Our strategy to investigate PCG measurements is the experimental reconstruction of the probabilities $p_{kl} \equiv p_l(\Psi_k)$. The relevant distribution to evaluate unbiasedness is the conditional probability $p_{l|k} = p_{kl}/\sum_l p_{kl}$ that the outcome of PCG measurements in momentum domain is l, given that $|\Psi_k\rangle$ was prepared. As a quantifier of unbiasedness, we calculate the entropy of the distribution $p_{l|k}$:

$$E_k = -\sum_{l=0}^{d-1} p_{l|k} \log_2(p_{l|k}). \tag{7}$$

Hence, unbiasedness is verified whenever $E_k = \log_2(d)$. In our setup, these outcome probabilities are obtained from the overall light power, W_{kl}, transmitted through the preparation and measurement spatial masks: $p_{l|k} = W_{kl}/\sum_l W_{kl}$. The transmitted light is monitored by an optical power meter (Newport 2931-C) set to output the mean value of 1000 power measurements performed over a total sampling time of 1s.

The upper part of Fig. 2 presents an example of the prepared beam intensity distribution and its corresponding Fraunhofer diffraction pattern. For this preparation, we used the periodic spatial mask $k = 0$, with bin width $s_x = 48\mu$m and $d = 4$, thus yielding a periodicity of $T_x = 192\mu$m. Following our notation, the prepared transverse field distribution corresponds to a quantum wave-function $\psi_0(x) = \langle x|\Psi_0\rangle$. This field distribution is optically Fourier transformed and the resulting Fraunhofer diffraction pattern is subjected to PCG measurements at the measurement site. The entropy E_0 associated with the outcome probabilities $p_{l|0}$ is given in Fig. 3(a) as a function of the PCG periodicities in momentum domain. Experimental data are shown as turquoise points while the solid orange line represents a theoretical prediction based on numerical calculations. The momentum periodicities $T_p = 2\pi d/(T_x m)$ arising from the unbiasedness condition (5) are indicated as dashed vertical lines. It is clear that for these specific values of the periodicity the entropy assumes either a maximum (when m is odd) or a minimum (when m is even). In Fig. 3(b), we show the measured distributions $p_{l|0}$ associated with the data points lying closer to these periodicities. For $d = 4$, the unbiasedness condition (5) is fulfilled for $m' = 1, 3$, as can be evidenced from the flat probability distribution $p_{l|0} \approx 1/d$ achieved for these periodicities.

The results presented in Fig. 3 illustrate unbiased PCG measurements of dimension 4 for the single preparation $|\Psi_0\rangle$. In order to fully demonstrate Eq. (2a), we also run our experiment with complementary preparations $|\Psi_k\rangle$ ($k = 0, \ldots, 3$). The extreme values obtained for the entropy E_k are indicated as error bars in Fig. 3(a). We find the values $E_k \geqslant 1.9953 \pm 0.0008 \,\forall\, k$ when using the periodicities associated with $m = 1$ and 3, thus demonstrating the full unbiasedness relation (2a) between preparation
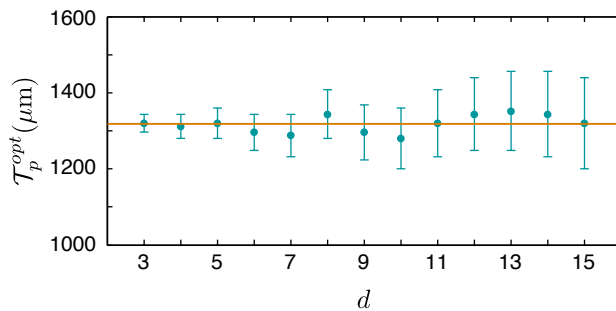
Figure 4: Measured optimal periodicity in momentum domain when using mask functions with constant bin width $s_x = 48\mu$m for the preparation of d-dimensional PCG. The theoretically predicted value is $\mathcal{T}_p^{opt} = f_e\lambda/s_x \approx 1319\mu$m.

and measurement outcomes for our periodic coarse graining. The presented error of 8×10^{-4} is due to fluctuations of the transmitted light power over 1000 measurements. This error is much smaller than the data points in Fig. 3(a). Finally, we note that the unitarity of the Fourier transformation (in mathematical terms, projection valued measures for position and momentum are unitarily equivalent [46]) and the functional dependence of condition (5) on the product of periodicities $T_x T_p$ (so they can be swapped), exempt the experimental verification of Eq. (2b) for the demonstration of mutual unbiasedness.

A few remarks on the resolution limitations of coarse-graining measurements are in order. The momentum periodicity T_p in plot 3(a) was scanned at the resolution limit of our setup: consecutive data points relate to bin widths differing by only 8μm (a single pixel of our SLM). This is the reason as to why the features shown in the theoretical prediction for smaller T_p could not be demonstrated experimentally. Theoretically, Eq. (5) provides an infinite number of possibilities for unbiasedness, but only a few are reachable in practice. The condition with $m = 1$ (valid for all d) offers the best trade-off between experimentally attainable resolutions in the position and momentum domains. In our optical setup, this trade-off implies the physical periodicity in the measurement SLM given by $\mathcal{T}_p = f_e\lambda d/T_x$, which for $d = 4$ and $T_x = 192\mu$m yields $\mathcal{T}_p \approx 1319\mu$m. The focal length f_e serves as a magnification parameter that can be used to adjust the momentum resolution at the cost of changing the detection range. Thus, a compromise between momentum resolution and a sensible detection range (the height of our SLM) also comes into play. An experimental investigation of this resolution trade-off in our optical setup is provided in the Supplemental Material [51].

As a final remark, the measurements shown in Fig. 4 illustrate a particular feature of Eq. (5). Keeping the preparation bin width at the constant value of $s_x = 48\mu$m, we looked for the optimal periodicities while varying the PCG measurement dimensionality from $d = 3$ up to 15. In this case, the condition for the optimal periodicity is independent of the dimension parameter d: $\mathcal{T}_p^{opt} = f_e\lambda/s_x \approx 1319\mu$m. The experimental uncertainty in its determination (the error bars) is dictated by the SLM pixel size: $\text{error}(\mathcal{T}_p^{opt}) = d \times 8\mu$m. Our measurements demonstrate close agreement with the theoretical prediction, as seen in Fig. 4. We obtain $|E_k - \log_2(d)| \lesssim 0.004$ for all data points, thus demonstrating unbiased coarse-grained measurements for dimensionality up to 15.

Discussion. We have shown how one can recover the condition of mutual unbiasedness in coarse-grained measurements of continuous variable systems. Periodic "mask" functions were used to define projective measurements in position and momentum variables, and these were shown to be mutually unbiased for particular combinations of periodicities. What other types of mask functions can form the MUBs and how do our findings complement the periodic-commuting case treated in its generality [54] are open questions on the theory side. Relevant, practically oriented questions also point towards the role of even values of m' and applications in interference experiments [55, 56]. Though (nonperiodic) coarse-grained observables have been used in quantum key distribution [60], application of the present scheme requires a careful security analysis, and is thus an open question for the future. Another interesting question is the use of our results in quadrature measurements, for which PCG might be implementable using auxiliary qubits, as in measurement of the parity operator [61]. Nontrivial coarse-graining structures have also been considered in the context of Bell inequalities violations [57–59]. Nonetheless, a formal demonstration of mutual unbiasedness was still missing in the general framework of CV measurements. We believe our results may provide a method to formally connect continuous and discrete variable quantum mechanics.

* Electronic address: dan.tasca@gmail.com
† Electronic address: rudnicki@cft.edu.pl

[1] J. Schwinger, Proc. Natl. Acad. Sci. **46**, 570 (1960).
[2] K. Kraus, Phys. Rev. D **35**, 3070 (1987).
[3] J. Sánchez, Phys. Lett. A **173**, 233 (1993).
[4] Z. Puchała, Ł. Rudnicki, K. Chabuda, M. Paraniak, and K. Życzkowski, Phys. Rev. A **92**, 032109 (2015).
[5] S. Cheng and M. J. W. Hall, Phys. Rev. A **92**, 042101 (2015).
[6] P. J. Coles, M. Berta, M. Tomamichel, and S. Wehner, Rev. Mod. Phys. **89**, 015002 (2017).
[7] A. Fernández-Pérez, A. B. Klimov, and C. Saavedra, Phys. Rev. A **83**, 052332 (2011).
[8] D. Giovannini, J. Romero, J. Leach, A. Dudley, A. Forbes, and M. J. Padgett, Phys. Rev. Lett. **110**, 143601 (2013).
[9] G. Vallone, D. G. Marangon, M. Tomasin, and P. Villoresi, Phys. Rev. A **90**, 052327 (2014).
[10] C. Spengler, M. Huber, S. Brierley, T. Adaktylos, and B. C. Hiesmayr, Phys. Rev. A **86**, 022311 (2012).
[11] E. C. Paul, D. S. Tasca, Ł. Rudnicki, and S. P. Walborn, Phys. Rev. A **94**, 012303 (2016).
[12] D. Sauerwein, C. Macchiavello, L. Maccone, and B. Kraus, Phys. Rev. A **95**, 042315 (2017).
[13] E. G. Cavalcanti, S. J. Jones, H. M. Wiseman, and M. D. Reid, Phys. Rev. A **80**, 032112 (2009).
[14] S. P. Walborn, A. Salles, R. M. Gomes, F. Toscano, and P. H. Souto Ribeiro, Phys. Rev. Lett. **106**, 130402 (2011).
[15] D. S. Tasca, Ł. Rudnicki, R. M. Gomes, F. Toscano, and S. P. Walborn, Phys. Rev. Lett. **110**, 210502 (2013).
[16] J. Schneeloch, P. B. Dixon, G. A. Howland, C. J. Broadbent, and J. C. Howell, Phys. Rev. Lett. **110**, 130407 (2013).
[17] J. Schneeloch, C. J. Broadbent, S. P. Walborn, E. G. Cavalcanti, and J. C. Howell, Phys. Rev. A **87**, 062103 (2013).
[18] P. Skrzypczyk and D. Cavalcanti, Phys. Rev. A **92**, 022354 (2015).
[19] M. Marciniak, A. Rutkowski, Z. Yin, M. Horodecki, and R. Horodecki, Phys. Rev. Lett. **115**, 170401 (2015).
[20] H. Zhu, M. Hayashi, and L. Chen, Phys. Rev. Lett. **116**, 070403 (2016).
[21] S. Pirandola et al., Nat. Photon. **9**, 397 (2015).
[22] M. Krenn, M. Malik, T. Scheidl, R. Ursin, and A. Zeilinger, *Quantum Communication with Photons* (Springer International Publishing, Cham, 2016), pp. 455–482.
[23] J. Bavaresco et al., arXiv:1709.07344v1 [quant-ph] (2017).
[24] A. C. Dada, J. Leach, G. S. Buller, M. J. Padgett, and E. Andersson, Nat. Phys. **7**, 677 (2011).
[25] V. Potoček, F. M. Miatto, M. Mirhosseini, O. S. Magaña Loaiza, A. C. Liapis, D. K. L. Oi, R. W. Boyd, and J. Jeffers, Phys. Rev. Lett. **115**, 160505 (2015).
[26] H.-K. Lau and M. B. Plenio, Phys. Rev. Lett. **117**, 100501 (2016).
[27] S. Takeda and A. Furusawa, *Optical Hybrid Quantum Information Processing* in *Principles and Methods of Quantum Information Technologies*, vol. 911 (Springer Lecture Note Phys., Tokyo, 2016).
[28] V. D. Salakhutdinov, E. R. Eliel, and W. Löffler, Phys. Rev. Lett. **108**, 173604 (2012).
[29] M. Krenn, M. Huber, R. Fickler, R. Lapkiewicz, S. Ramelow, and A. Zeilinger, Proc. Natl. Acad. Sci. U.S.A. **111**, 6243 (2014).
[30] I. B. Bobrov, E. V. Kovlakov, A. A. Markov, S. S. Straupe, and S. P. Kulik, Opt. Express **23**, 649 (2015).
[31] S. Restuccia, D. Giovannini, G. Gibson, and M. Padgett, Opt. Express **24**, 27127 (2016).
[32] L. Neves, G. Lima, E. J. S. Fonseca, L. Davidovich, and S. Pádua, Phys. Rev. A **76**, 032314 (2007).
[33] G. Cañas, N. Vera, J. Cariñe, P. González, J. Cardenas, P. W. R. Connolly, A. Przysiezna, E. S. Gómez, M. Figueroa, G. Vallone, et al., Phys. Rev. A **96**, 022317 (2017).
[34] C. Schaeff, R. Polster, R. Lapkiewicz, R. Fickler, S. Ramelow, and A. Zeilinger, Opt. Express **20**, 16145 (2012).
[35] Z. Xie, T. Zhong, S. Shrestha, X. Xu, J. Liang, Y.-X. Gong, J. C. Bienfang, A. Restelli, J. H. Shapiro, W. N. C., et al., Nat. Photon. **9**, 536 (2015).
[36] Ł. Rudnicki, S. P. Walborn, and F. Toscano, EPL **97**, 38003 (2012).
[37] Ł. Rudnicki, S. P. Walborn, and F. Toscano, Phys. Rev. A **85**, 042115 (2012).
[38] M. R. Ray and S. J. van Enk, Phys. Rev. A **88**, 042326 (2013).
[39] M. R. Ray and S. J. van Enk, Phys. Rev. A **88**, 062327 (2013).
[40] T. Durt, B.-G. Englert, I. Bengtsson, and K. Życzkowski, Int. J. Quant. Inf. **08**, 535 (2010).
[41] A. Kalev and G. Gour, New. J. Phys. **16**, 053038 (2014).
[42] S. Weigert and M. Wilkinson, Phys. Rev. A **78**, 020303 (2008).
[43] F. Schlederer, M. Krenn, R. Fickler, M. Malik, and A. Zeilinger, New J. Phys. **18**, 043019 (2016).
[44] A. Babazadeh, M. Erhard, F. Wang, M. Malik, R. Nouroozi, M. Krenn, and A. Zeilinger, arXiv:1702.07299 [quant-ph] (2017).
[45] A. F. L. Accardi and V. Gorini, *Some trends and problems in quantum probability* in *Quantum Probability and Applications to the Quantum Theory of Irreversible Processes*, vol. 1055 (Springer Lecture Note Math., New York, 1984).
[46] G. Cassinelli and V. S. Varadarajan, Quantum Probability and Related Topics **5**, 135 (2002).
[47] D. S. Tasca, Ł. Rudnicki, R. S. Aspden, M. J. Padgett, P. H. Souto Ribeiro, and S. P. Walborn, arXiv:1506.01095 [quant-ph] (2015).
[48] Y. Aharonov, H. Pendleton, and A. Peterson, Int. J. Theor. Phys. **2**, 213 (1969).
[49] P. Busch and P. J. Lahti, Phys. Lett. A **115**, 259 (1986).
[50] H. Reiter and W. Thirring, Found. Phys. **19** , 1037 (1989).
[51] D. S. Tasca, P. Sánchez, S. P. Walborn, and Ł. Rudnicki, Supplemental Material for *Mutual unbiasedness in coarse-grained continuous variables* (2017).
[52] Ł. Rudnicki, D. S. Tasca, and S. P. Walborn, Phys. Rev. A **93**, 022109 (2016).

[53] D. Marcuse, *Light Transmission Optics* (Van Nostrand Reinhold, New York, 1982).

[54] K. Ylinen, J. Math. Analy. Applic. **137**, 185 (1989).

[55] J. C. G. Biniok and P. Busch, Phys. Rev. A **87**, 062116 (2013).

[56] J. C. G. Biniok, P. Busch, and J. Kiukas, Phys. Rev. A **90**, 022115 (2014).

[57] J. Wenger, M. Hafezi, F. Grosshans, R. Tualle-Brouri, and P. Grangier, Phys. Rev. A **67**, 012105 (2003).

[58] D. Cavalcanti, N. Brunner, P. Skrzypczyk, A. Salles, and V. Scarani, Phys. Rev. A **84**, 022105 (2011).

[59] M. T. Quintino, M. Araújo, D. Cavalcanti, M. F. Santos, and M. T. Cunha, J. Phys. A **45**, 215308 (2012).

[60] S. P. Walborn, D. S. Lemelle, M. P. Almeida, and P. H. Souto Ribeiro, Phys. Rev. Lett. **96**, 090501 (2006).

[61] L. G. Lutterbach, and L. Davidovich, Phys. Rev. Lett. **78**, 2547–2550 (1997).

[62] Mutually unbiased measurements are projective only in the limiting case when they describe the MUBs.

[63] We assume that 0 does not belong to $\mathbb{N}$.

[64] Our actual Lab setup uses double passage by a single SLM whose screen is divided into two sections for preparation and measurement parts of the experiment. Our device is a HOLOEYE PLUTO-NIR-015 phase-only spatial light modulator.

Supplemental Material for *Mutual Unbiasedness in Coarse-grained Continuous Variables*

Daniel S. Tasca,[1, *] Piero Sánchez,[2] Stephen P. Walborn,[3] and Łukasz Rudnicki[4, 5, †]

[1]*Instituto de Física, Universidade Federal Fluminense, Niteroi, RJ 24210-346, Brazil*
[2]*Departamento de Ciencias, Sección Física, Pontificia Universidad Católica del Perú, Apartado 1761, Lima, Peru*
[3]*Instituto de Física, Universidade Federal do Rio de Janeiro,*
Caixa Postal 68528, Rio de Janeiro, RJ 21941-972, Brazil
[4]*Max-Planck-Institut für die Physik des Lichts, Staudtstraße 2, 91058 Erlangen, Germany*
[5]*Center for Theoretical Physics, Polish Academy of Sciences, Al. Lotników 32/46, 02-668 Warsaw, Poland*

I. EXPLICIT DERIVATION OF EQ. (6) OF THE MAIN TEXT

The aim of this section is to express $p_l(\Psi) = \langle \Psi | \Omega_l | \Psi \rangle$ defined by

$$\Omega_l = \int_{\mathbb{R}} dp M_l (p - p_{\text{cen}}; T_p) |p\rangle \langle p|, \tag{S1}$$

with

$$M_k(z; T) = \begin{cases} 1, & k\,s \leq z\,(\text{mod T}) < (k+1)s \\ 0, & \text{otherwise} \end{cases}, \qquad k = 0, \ldots, d-1, \tag{S2}$$

in terms of the position wave-function $\psi(x) = \langle x | \Psi \rangle$. Note that, by definition

$$p_l(\Psi) = \int_{\mathbb{R}} dp M_l (p - p_{\text{cen}}; T_p) \tilde{\rho}(p), \tag{S3}$$

where $\tilde{\rho}(p) = |\tilde{\psi}(p)|^2$ and $\tilde{\psi}(p) = \langle p | \Psi \rangle$.

To achieve the desired goal we first represent the periodic mask function in terms of its Fourier decomposition

$$M_k(z; T) = \sum_{N \in \mathbb{Z}} \frac{1 - e^{-\frac{2\pi i N}{d}}}{2\pi i N} e^{-\frac{2\pi i N}{d} k} e^{\frac{2\pi i N}{T} z} \equiv \frac{1}{d} + \sum_{N \in \mathbb{Z}/\{0\}} \frac{1 - e^{-\frac{2\pi i N}{d}}}{2\pi i N} e^{-\frac{2\pi i N}{d} k} e^{\frac{2\pi i N}{T} z}. \tag{S4}$$

Clearly

$$p_l(\Psi) = \frac{1}{d} + \sum_{N \in \mathbb{Z}/\{0\}} \frac{1 - e^{-\frac{2\pi i N}{d}}}{2\pi i N} e^{iN\phi_l} \int_{\mathbb{R}} dp\, e^{\frac{iN\tau_p}{\hbar} p} \tilde{\rho}(p), \tag{S5}$$

with $\phi_l = -2\pi l/d - p_{\text{cen}}\tau_p/\hbar$ and $\tau_p = 2\pi\hbar/T_p$. The momentum integral gives the characteristic function of the momentum probability distribution, $\tilde{\Phi}(N\tau_p/\hbar)$, defined as

$$\tilde{\Phi}(\lambda) = \int_{\mathbb{R}} dp\, e^{i\lambda p} \tilde{\rho}(p). \tag{S6}$$

The autocorrelation form of the characteristic function reads [1]:

$$\tilde{\Phi}(\lambda) = \int_{\mathbb{R}} dx \psi^*(x) \psi(x + \hbar\lambda). \tag{S7}$$

Note that Eq. 3 from [1] deals with the characteristic function of position probability distribution, so that the shift $\hbar\lambda$ appears with the minus sign. The formula (S7) is a simple consequence of the Fourier transformation between wave functions in both domains. As a final result we obtain the desired expression

$$p_l(\Psi) = \frac{1}{d} + \sum_{N \in \mathbb{Z}/\{0\}} \frac{1 - e^{-\frac{2\pi i N}{d}}}{2\pi i N} e^{iN\phi_l} \int_{\mathbb{R}} dx \psi^*(x) \psi(x + N\tau_p). \tag{S8}$$

II. RESOLUTION TRADE-OFF IN PERIODIC COARSE GRAINING

To illustrate the capability of our setup to implement unbiased PCG measurements, we run our system further with increased mask periodicities in the preparation SLM. For each chosen T_x, we look for the entropy peak associated with condition $m = 1$ and experimentally determine the optimal periodicity $\mathcal{T}_p^{opt}$ at the measurement site. These results are displayed in Fig. S1 for $d = 4$ and 7. In all measurements, we obtain optimal periodicities very close to the theoretical prediction (solid orange curve), the uncertainty in its determination (the error bars) being dictated by SLM pixel size: $\mathrm{error}(\mathcal{T}_p^{opt}) = d \times 8\mu$m. For both dimensions, all obtained entropies are indicative of unbiased measurement outcomes: $E_k \geqslant 1.997 \pm 0.001 \ (\approx \log_2 4)$ or $E_k \geqslant 2.799 \pm 0.001 \ (\approx \log_2 7)$.
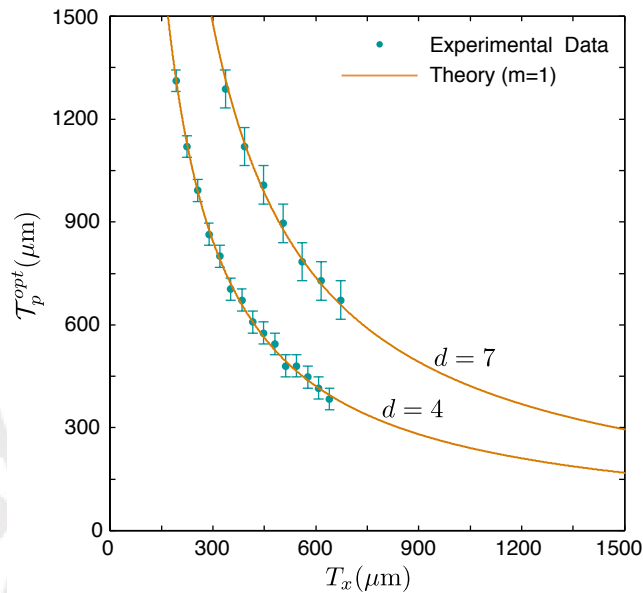
FIG. S1: Experimental demonstration of the resolution trade-off between the pair of periodicities in position and momentum domain leading to unbiased PCG measurements with $d = 4$ and $d = 7$.

* Electronic address: dan.tasca@gmail.com
† Electronic address: rudnicki@cft.edu.pl
[1] Ł. Rudnicki, D. S. Tasca, and S. P. Walborn, Phys. Rev. A **93**, 022109 (2016).

Mutual Unbiasedness in Coarse-grained Continuous Variables

Piero Sánchez Melgar

Table of contents

Introduction

- For Mutually Unbiased Bases (MUB), preparation in the first basis leads to equal probability (loss of information) of states in the second basis.

- The usual coarse-grained measurements break the mutual unbiasedness between conjugate continuous variables (transverse position-x and momentum-P_x of a paraxial beam).

- Using Periodic Coarse Graining (PCG) we can achieve this unbiasedness for a specific configuration (MUB condition).

Mutually Unbiased Bases (MUB)

When silver atoms pass through a Stern-Gerlach device (z-axis), the magnetic field gradient deflects half of them up and half down (on average) depending on each atom's spin. This prepares the spin state in an eigenstate of Z.
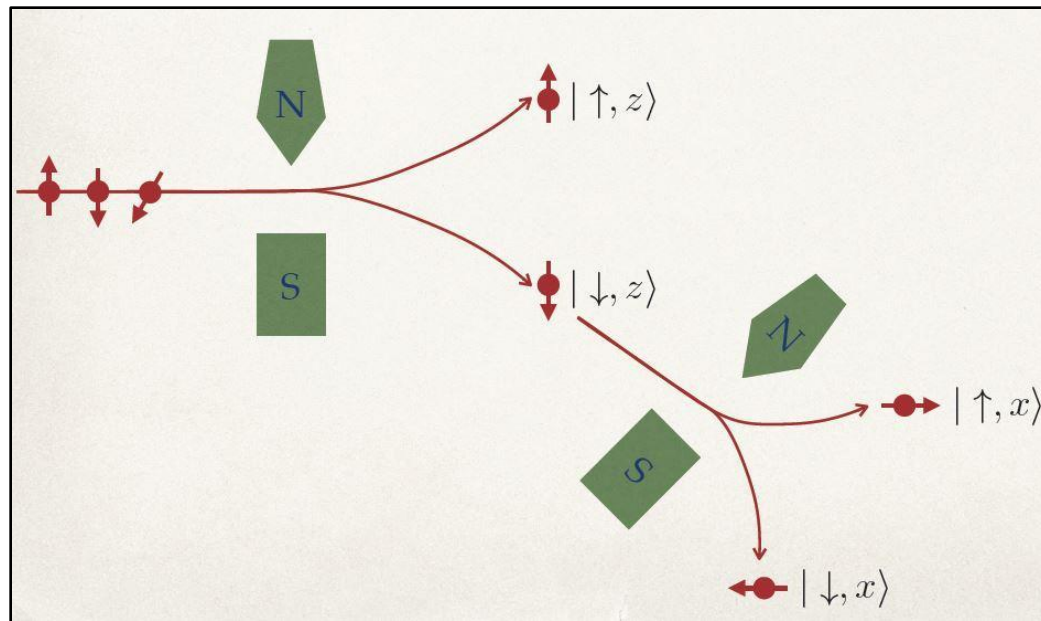
$$\mathcal{B}_z = \{|\uparrow, z\rangle, |\downarrow, z\rangle\}$$
$$\mathcal{B}_x = \{|\uparrow, x\rangle, |\downarrow, x\rangle\}$$
$$\mathcal{B}_y = \{|\uparrow, y\rangle, |\downarrow, y\rangle\}$$

$$|\langle\uparrow, x|\downarrow, z\rangle|^2 = 1/2$$

$$|\langle\downarrow, x|\downarrow, z\rangle|^2 = 1/2$$

If one of these states enters a second device aligned with an orthogonal axis (spin measured in the X basis), again, half is deflected up and half down (on average). This means we lost all information about the starting state's spin and these two-dimensional bases are said to be mutually unbiased

Mutually Unbiased Bases (MUB)

In a more general case of two $\boldsymbol{d}$-dimensional mutually unbiased bases (MUB):

$$\{|a_0\rangle, |a_1\rangle, \dots, |a_{d-1}\rangle\}$$

$$\{|b_0\rangle, |b_1\rangle, \dots, |b_{d-1}\rangle\}$$

$$\Longrightarrow \quad |\langle a_i | b_j \rangle|^2 = \frac{1}{d}$$

There is also the case of continuous variables $\hat{\boldsymbol{x}}$ and $\hat{\boldsymbol{p}}$ with $[\hat{\boldsymbol{x}}, \hat{\boldsymbol{p}}] = i\hbar$. This means they are conjugate variables, so one is the Fourier transform of the other and they form MUB:

$$Position: \quad \{\,|x\rangle\,\}$$

$$Momentum: \quad \{\,|p\rangle\,\}$$

$$\Longrightarrow \quad \langle x | p \rangle = \frac{e^{ipx/\hbar}}{\sqrt{2\pi\hbar}}$$

$$|\langle x | p \rangle|^2 = \frac{1}{2\pi\hbar}$$

MUB are useful in the field of Quantum Information. Some applications include quantum state tomography and quantum cryptography.

Standard Coarse Graining

Heisenberg's uncertainty principle:

$$\Delta x \Delta p \geq \frac{\hbar}{2}$$

The usual coarse-grained position-momentum measurements use projectors:

$$A_k = \int_{k_-\Delta}^{k_+\Delta} dx \, |x\rangle \langle x| \qquad B_l = \int_{l_-\delta}^{l_+\delta} dp \, |p\rangle \langle p|$$

$$k, l \in \mathbb{Z}$$
$$k_\pm = k \pm 1/2$$
$$l_\pm = l \pm 1/2$$

A quantum state localized in the first basis <u>is not</u> evenly spread with respect to the second basis but instead decays like the sinc function

$$\psi(x) = \frac{1}{\sqrt{\Delta}}$$

$$for \; |x| \leq \frac{\Delta}{2}$$

FOURIER TRANSFORM
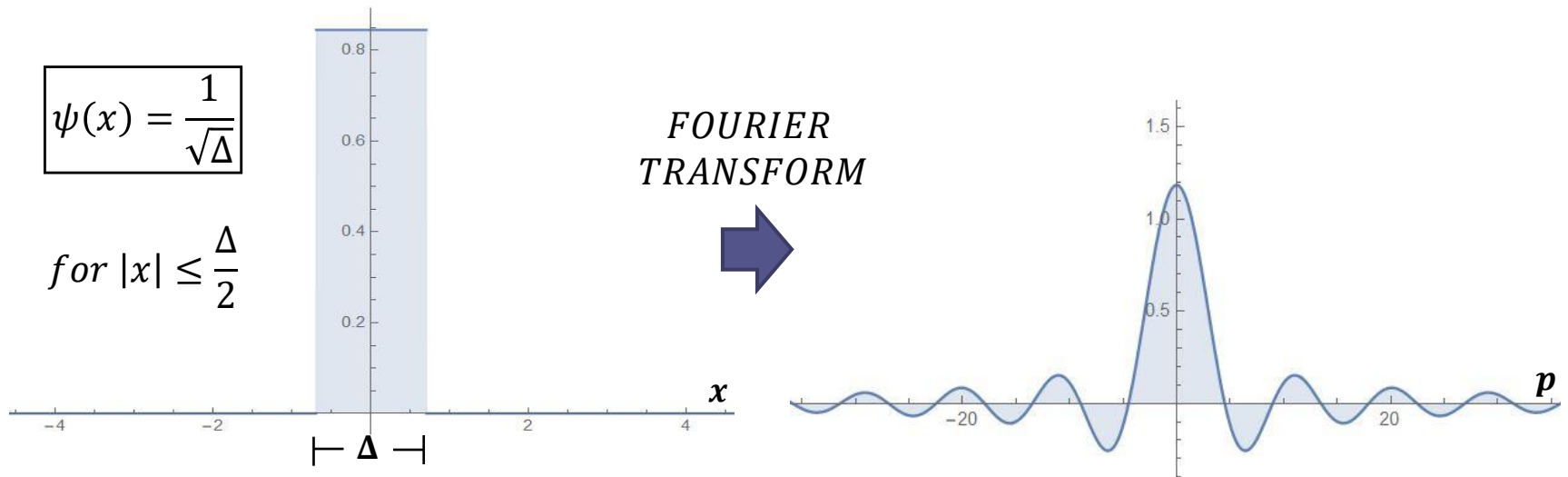
Periodic Coarse Graining (PCG)

- The PCG of a continuous variable (CV) "z" is specified by the measurement setting (z_0, d, T_z). This generates a set $\{M_k(z - z_0; T_z)\}$ of d mask functions with bin width $s_z = T_z/d$

- We define measurement operators for the conjugate CV "x" and "p":

$$\hat{\Pi}_k = \int_{\mathbb{R}} dx\, M_k(x - x_0, T_x)|x\rangle\langle x|, \quad \hat{\Omega}_k = \int_{\mathbb{R}} dp\, M_k(p - p_0, T_p)|p\rangle\langle p|,$$
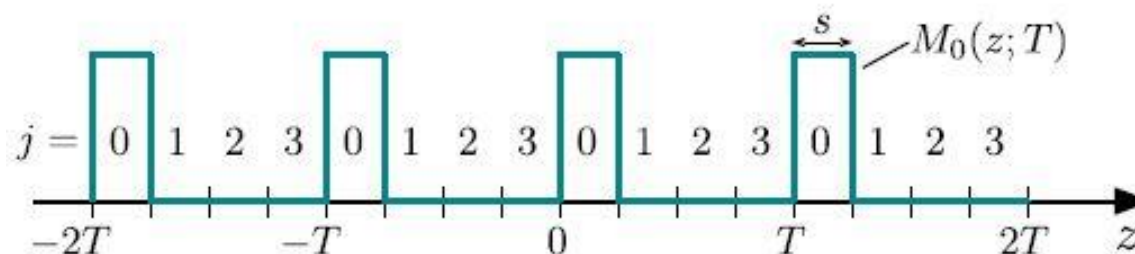
- Eigenfunction: $\quad \hat{\Pi}_k|\psi_k\rangle = |\psi_k\rangle$

$$\psi_k(x) = \frac{1}{N}h(x)M_k(x - x_0, T_x)$$

k = 0, ... , d-1
N: normalization constant
h(x): gaussian function

Intensity profile
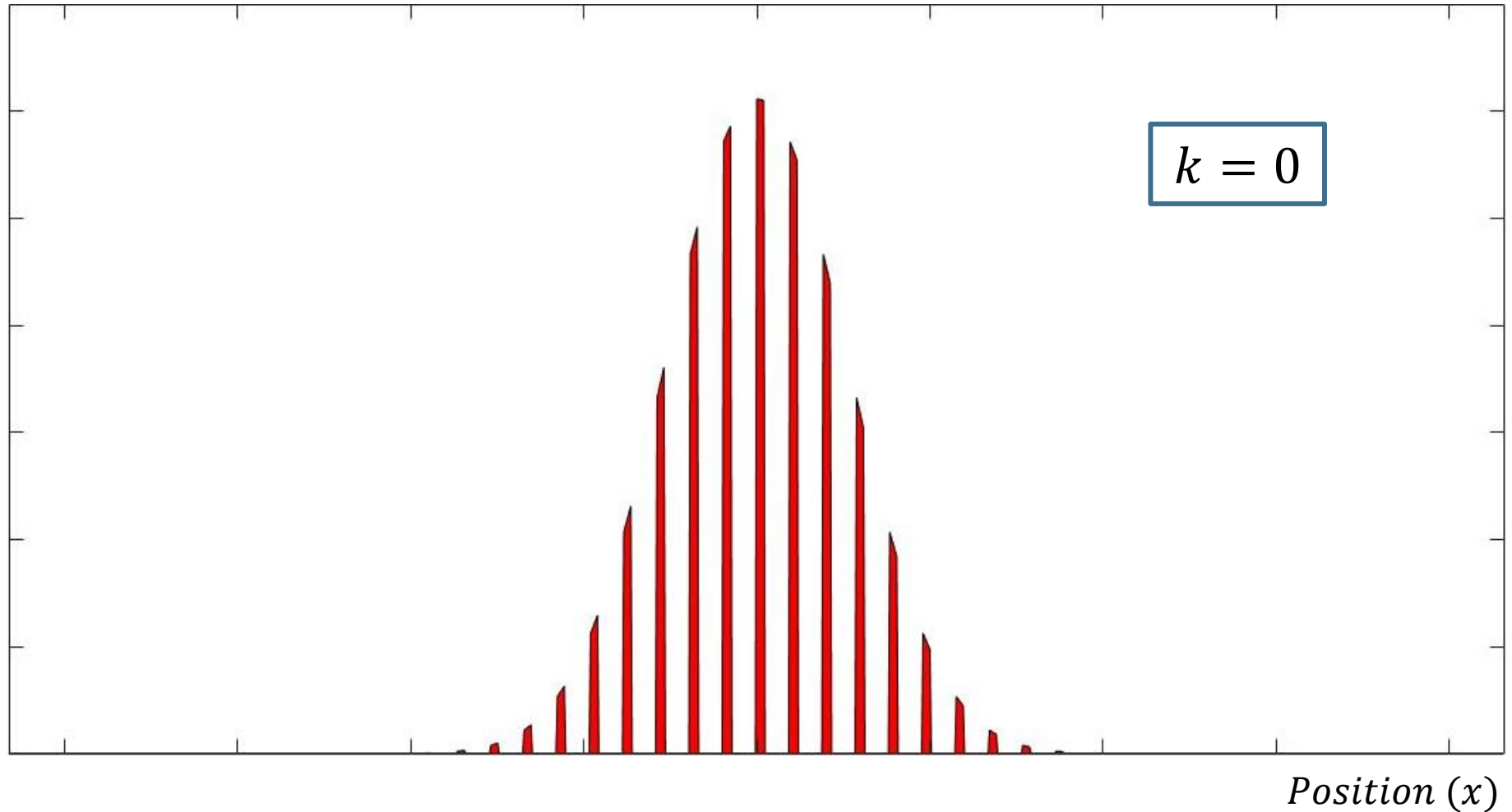
Intensity (I)

$k = 0$

Position (x)

Intensity profile

Intensity (I)

$$k = 1$$

Position (x)

Intensity profile

Intensity (I)

$$k = 2$$

Position (x)
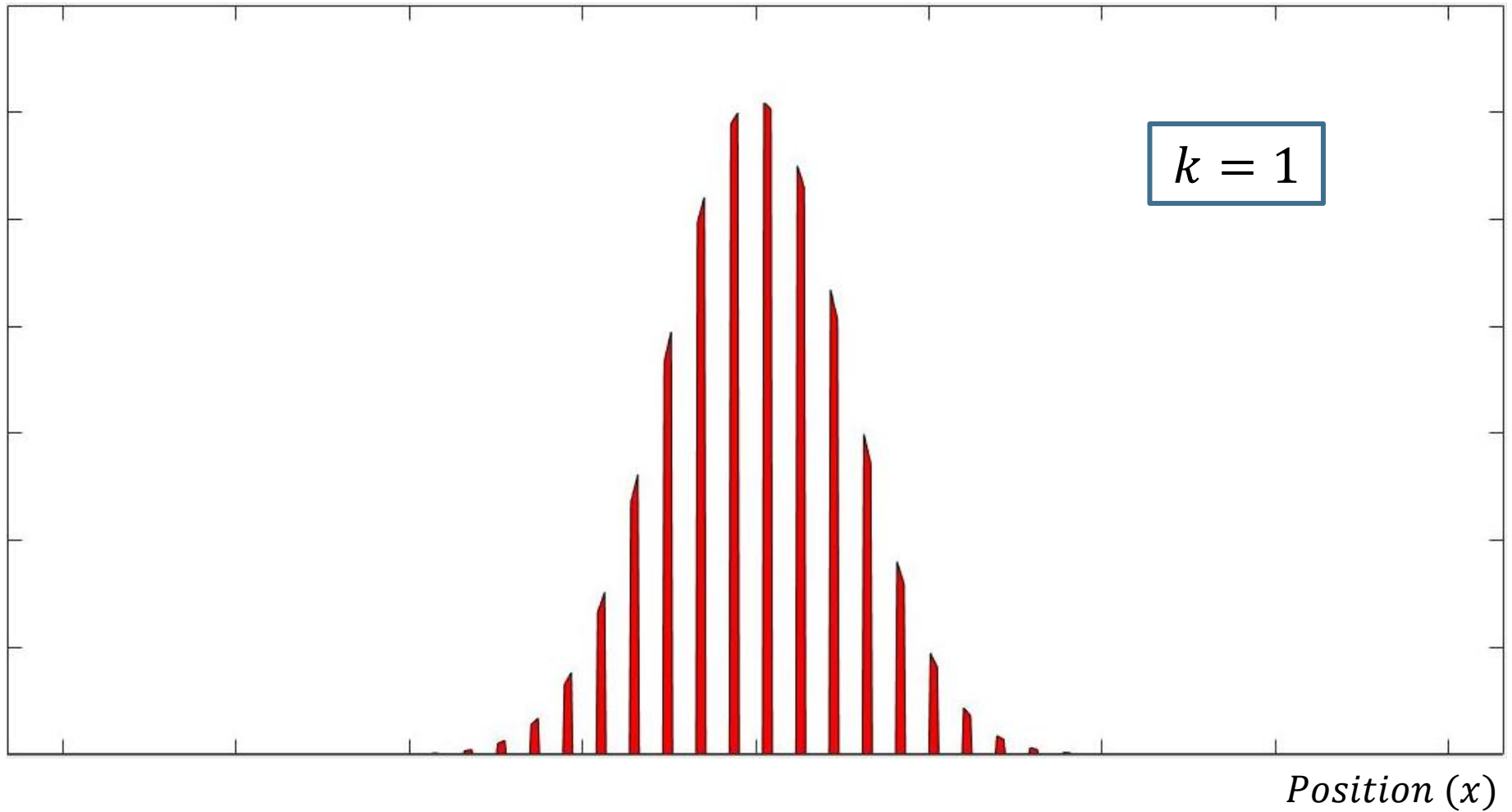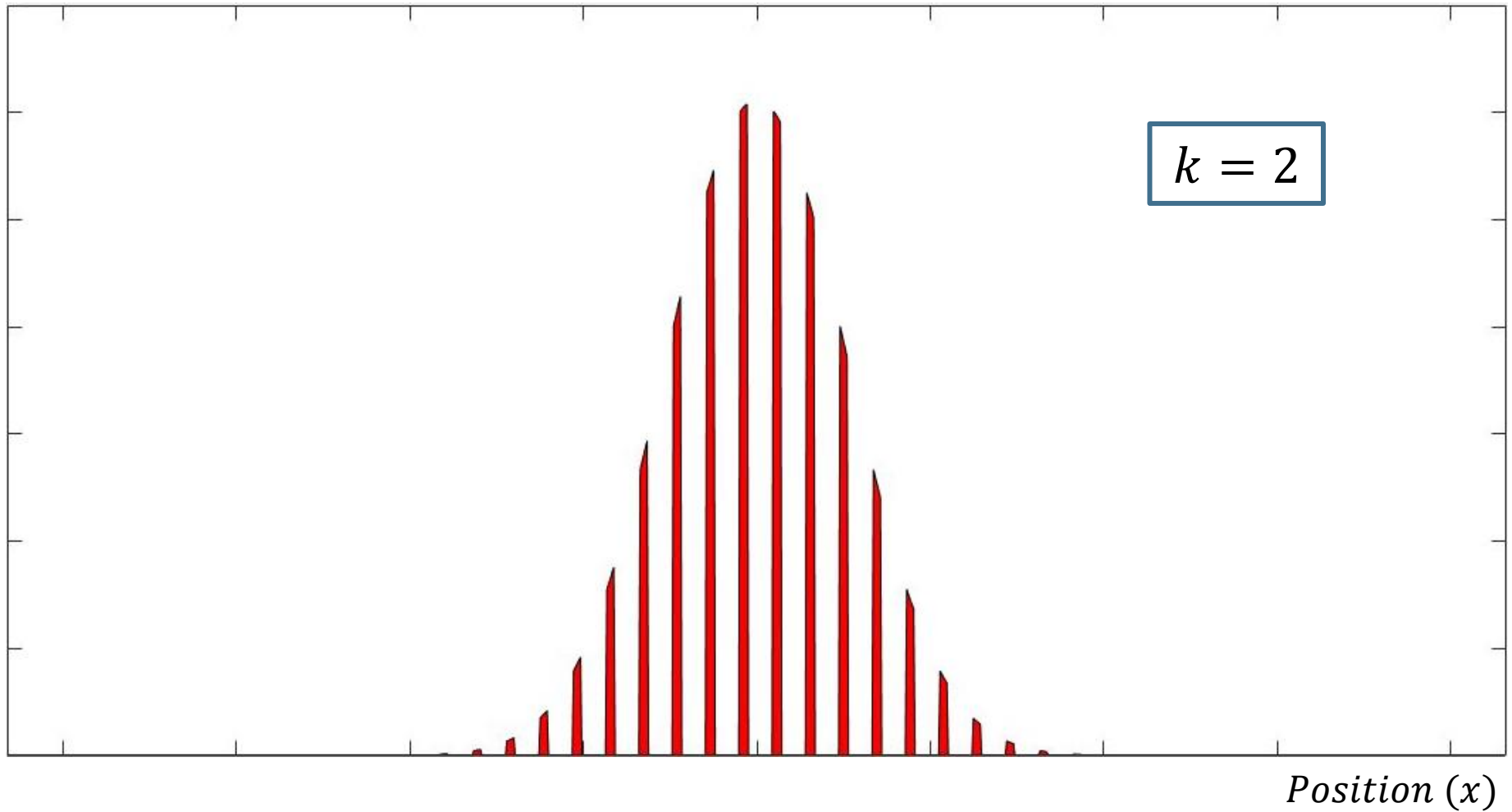
Mutually Unbiased Measurements (MUM)

- MUM for PCG require:

$$\langle \psi_k | \hat{\Omega}_l | \psi_k \rangle = \frac{1}{d}$$

$$\langle \phi_k | \hat{\Pi}_l | \phi_k \rangle = \frac{1}{d}$$

- General measurements for PCG:

$$\langle \psi_k | \hat{\Omega}_l | \psi_k \rangle = p_{l|k}(h, T_x, T_p, p_0, d)$$

$$\langle \phi_k | \hat{\Pi}_l | \phi_k \rangle = p_{l|k}(h, T_x, T_p, x_0, d)$$

for any $k, l \in \{0, \dots, d-1\}$ with $0 \le p_{l|k} \le 1$

- We want to prove that:

$$p_{l|k}(h, T_x, T_p = 2\pi d T_x^{-1}, p_0, d) = \frac{1}{d}$$

- First theoretical MUB condition:

- Experimentally we found:

$$\boxed{\begin{aligned} T_x T_p &= 2\pi d \\ T_x T_p &= \frac{2\pi d}{m} \end{aligned}}$$

$(\hbar = 1)$

Main experimental setup

$$T_x T_p = 2\pi d$$
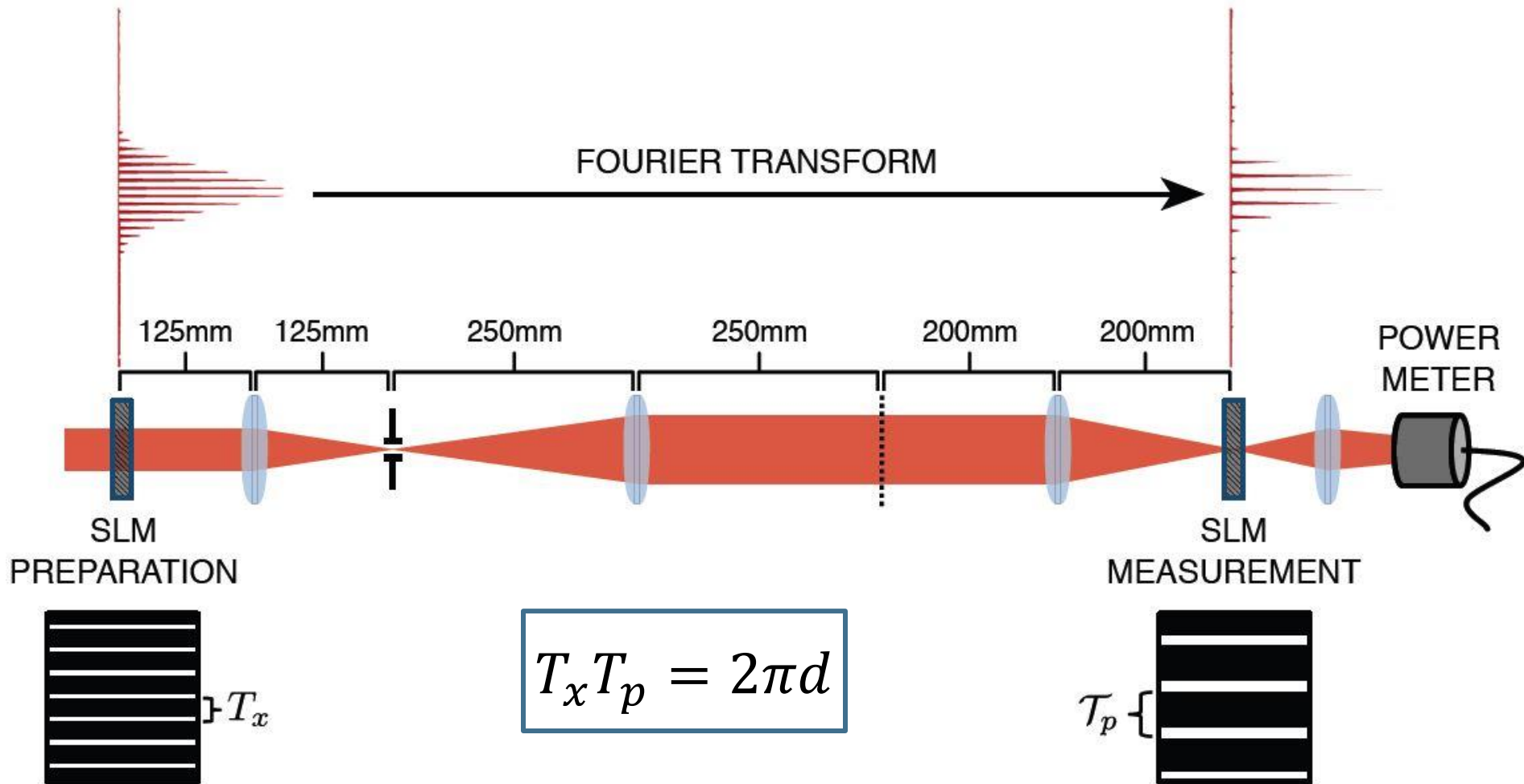
Main experimental setup

The measurement SLM is in the Fourier plane, but we measure in units of length, not momentum. The period T_p is reinterpreted:

$$T_p = \left(\frac{f_e \lambda}{2\pi}\right) \mathcal{T}_p$$

$f_e : Effective\ focal\ length$
$\lambda : Beam\ wavelength$

So the main condition we want to prove changes with the setup parameters:

$$T_x T_p = 2\pi d$$

$$\boxed{T_x \mathcal{T}_p = f_e \lambda d} \quad or \quad \boxed{s_x s_p = \frac{f_e \lambda}{d}}$$

MUB condition

$(T_j = s_j d)$

Main experimental setup

The relation between the focal lengths is:

$$f_e = \frac{f_1 f_3}{f_2}$$

There are some constraints for this setup:

- Because of the limited SLM screen size: $f_e = 100\ mm$

- In order to not obstruct beams near the SLM: $f_3 = 200\ mm$

Therefore, the relation between the focal lengths of the first two lenses is:

$$\frac{f_1}{f_2} = \frac{1}{2}$$

$f_1 = 125\ mm$

$f_2 = 250\ mm$

Intensity measurement

- To evaluate the unbiasedness of the measurements, we measure the intensities (corresponding to probabilities):

$$\langle \psi_k | \hat{\Omega}_l | \psi_k \rangle = p_{l|k}(h, T_x, T_p, p_0, d) \qquad \text{for each } \boldsymbol{k}, \boldsymbol{l} \in \{\boldsymbol{0}, \dots, \boldsymbol{d-1}\}$$

- We calculate the conditional probability distributions $\boldsymbol{p_{l|k} = p_{kl}/p_k}$ of measuring the $\boldsymbol{l}$ mask if only the $\boldsymbol{k}$ mask was prepared

$d = 4$

$l \rightarrow$ 0 1 2 3

k 0 1 2 3

each row gives

$\boldsymbol{d \times d \ probability \ matrix}$

$\boldsymbol{p_{l|k}}$

Not at MUB condition

$\boldsymbol{p_{l|k}}$

$1/d$
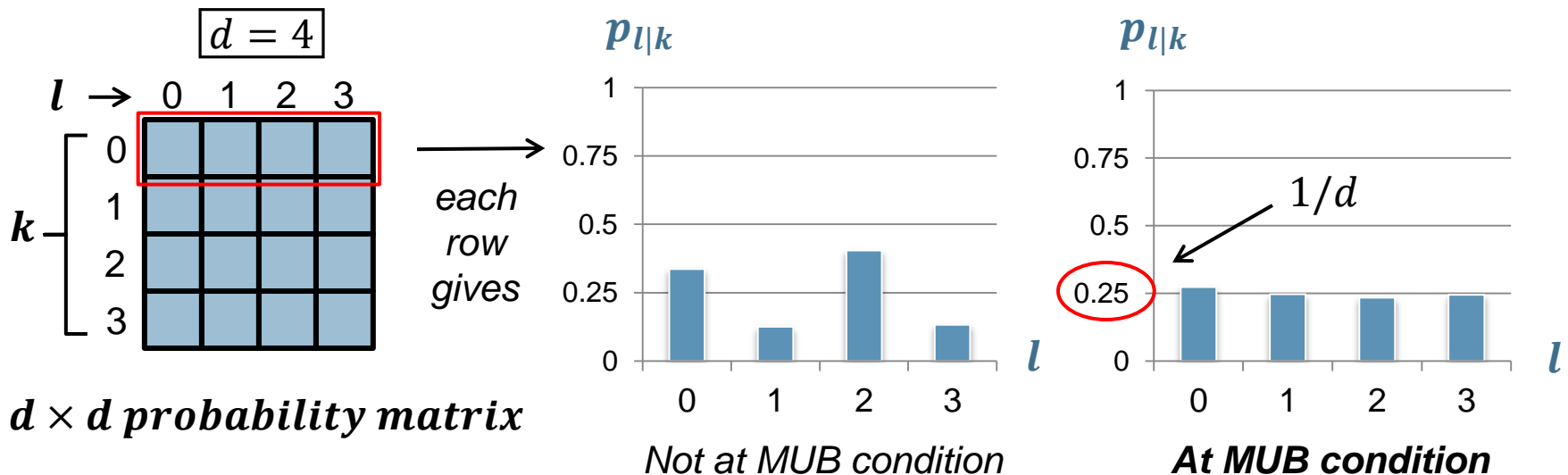
At MUB condition

Entropy measurement

- Then we calculate the Shannon entropy of one row of the matrix:

$$E_k = -\sum_{l=0}^{d-1} p_{l|k} \log_2(p_{l|k}) \quad \xrightarrow[\text{Maximum entropy}]{\text{MUB condition}} \quad \boxed{E_k = \log_2(d)}$$

- We use this as an indicator of unbiasedness and repeat the process for different configurations of $\mathcal{T}_p, T_x$ and d.

- We used the HOLOEYE PLUTO-NIR-015 phase-only spatial light modulator with the Newport 2931-C powermeter.

Calibration of the SLM

We used a phase-only spatial light modulator (SLM), a device that adds a phase ($\phi(g)$) to the incident beam depending on the shade of gray (g) projected. The SLM is aligned in such a way that only the horizontally polarized light is affected:

$$|H\rangle \rightarrow e^{i\phi(g)}|H\rangle$$
$$|V\rangle \rightarrow |V\rangle$$

We prepare the diagonally polarized state: $\qquad |\psi_0\rangle = \dfrac{|H\rangle + |V\rangle}{\sqrt{2}}$

By changing the parameter g, we transform the state: $\qquad |\psi_{SLM}\rangle = \dfrac{e^{i\phi(g)}|H\rangle + |V\rangle}{\sqrt{2}}$

Then, we project this state with $|\psi_0\rangle$ and measure the intensity, which allows us to obtain $\phi(g)$. We want this increment in phase to be <u>linear</u> with respect to the shade of gray projected, so we adjust g accordingly using a <u>blazing function</u>.

Calibration of the SLM

$$|\psi_0\rangle = \frac{|H\rangle + |V\rangle}{\sqrt{2}}$$

$$|\psi_{SLM}\rangle = \frac{e^{i\phi(g)}|H\rangle + |V\rangle}{\sqrt{2}}$$

PBS **HWP(22.5°)** **SLM** **HWP(22.5°)** **PBS** **PM**
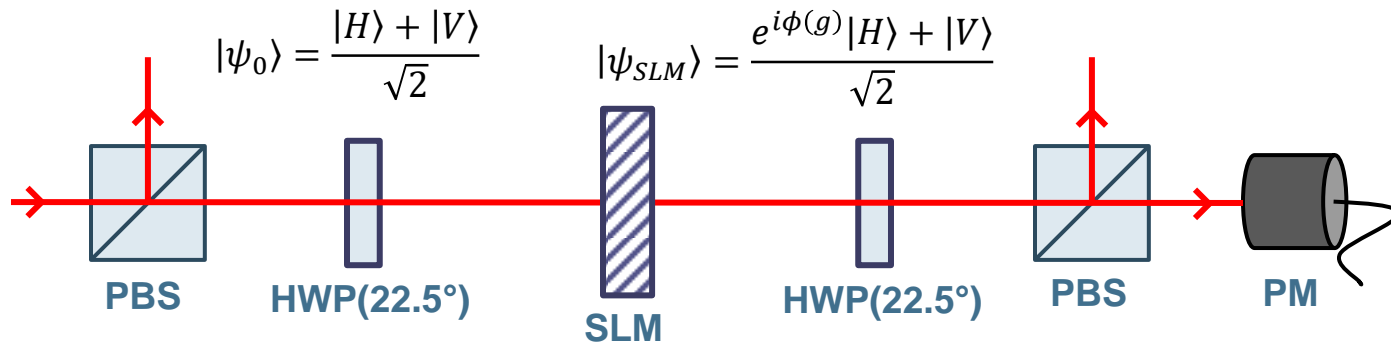
$$\frac{I(g)}{I_{MAX}} = |\langle\psi_0|\psi_{SLM}\rangle|^2 = \left|\left(\frac{\langle H| + \langle V|}{\sqrt{2}}\right)\left(\frac{e^{i\phi(g)}|H\rangle + |V\rangle}{\sqrt{2}}\right)\right|^2$$

$$= \left|\frac{e^{i\phi(g)} + 1}{2}\right|^2 = cos^2\left(\frac{\phi(g)}{2}\right) \Rightarrow \boxed{\phi(g) = 2\,cos^{-1}\left(\sqrt{\frac{I(g)}{I_{MAX}}}\right)}$$

Calibration of the SLM

- Blazing funtion:
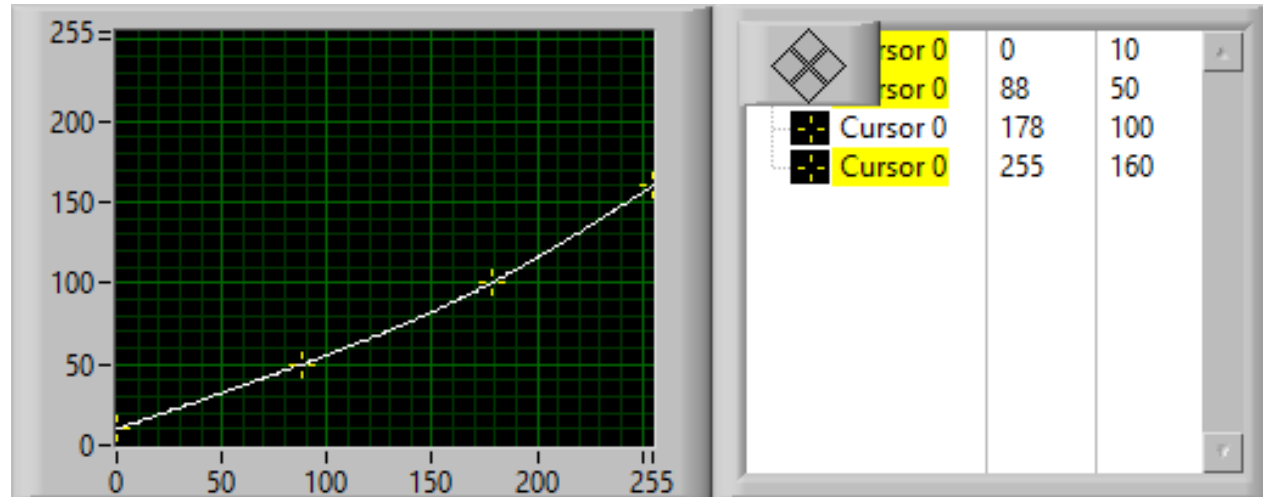
- Final result:

Intensity

Phase / π

Gray Level

Gray Level
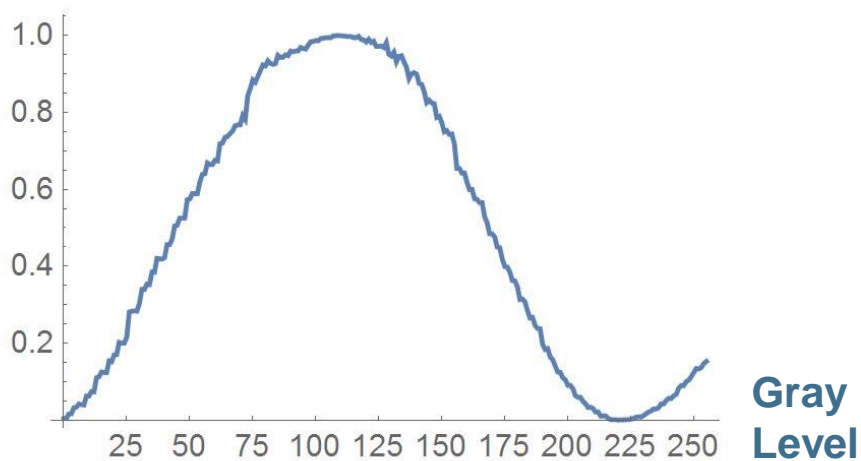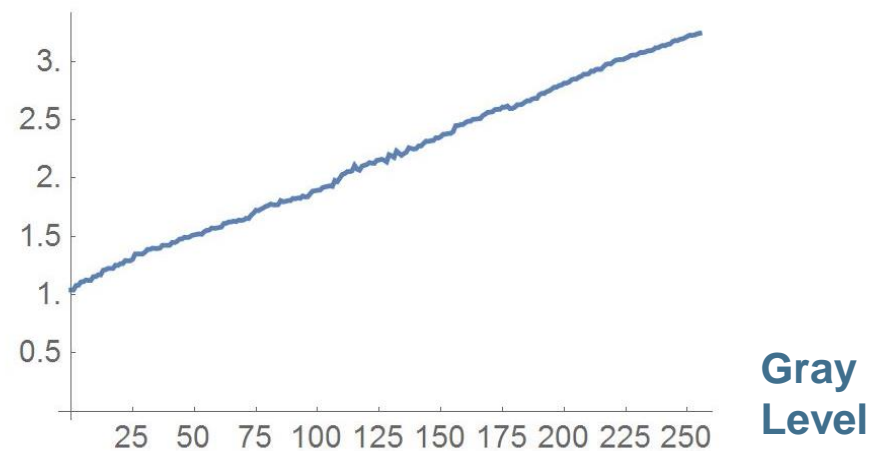
Diffraction grating

We can use the SLM to simulate a diffraction grating by projecting a periodic ramp function along one axis of the screen. This will generate different orders of diffraction in the Fourier plane that are separated from each other.
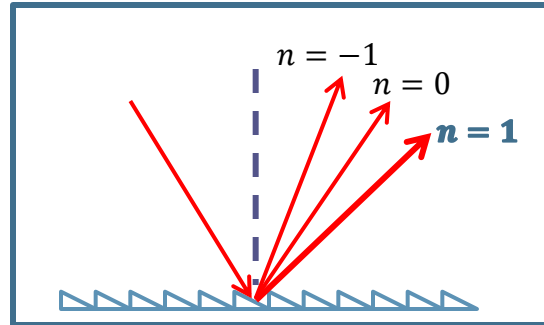

The first order diffraction is the one with the highest intensity and by filtering it we keep only the modulated light to use in the experiment. The efficiency is obtained by comparing the intensity in the first and zeroth order diffraction.

By using this diffraction grating only in certain sections of the SLM, we can effectively "cut" the beam in different patterns, which will be useful in the preparation of our experimental state.

Diffraction grating

Phase / π

$$\Phi_{xShift}(x,y) = (2\pi x / \Lambda_x) \bmod 2\pi$$

$\vdash \Lambda_x \dashv$

X

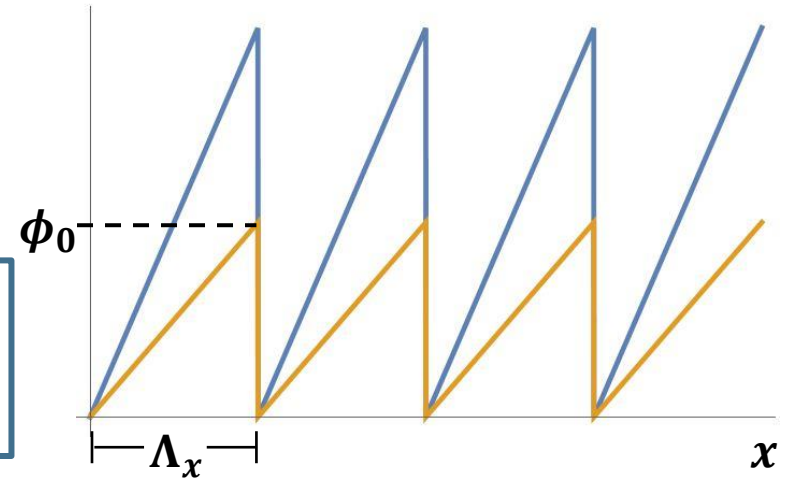**Prism** **SLM screen**

lateral shift
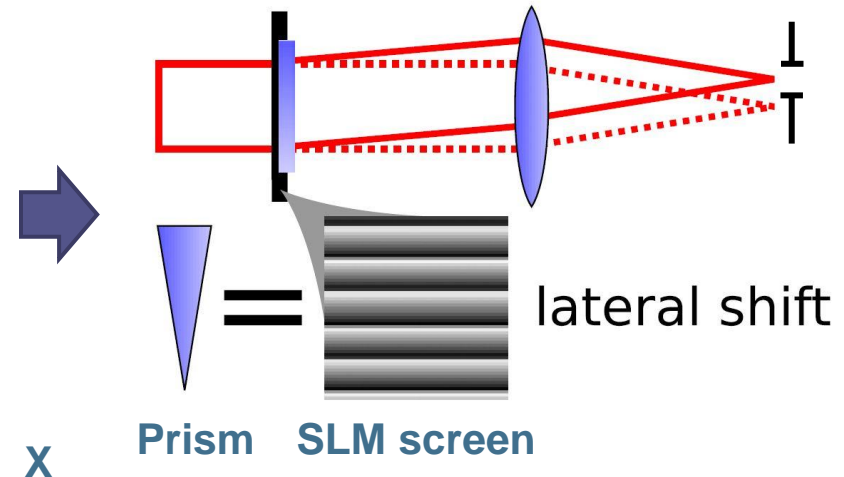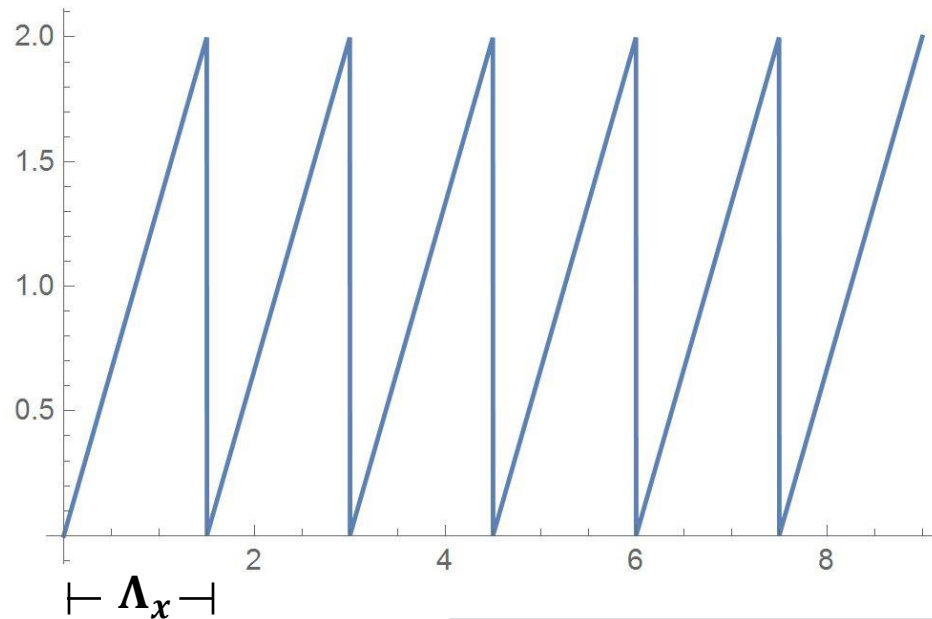
- Experimental **first-order** diffraction efficiency: $\dfrac{I_1}{I_0} \times 100\% = 73.8\,\%$

Diffraction grating

Theoretical case with a phase up to $\boldsymbol{\phi_0}$

$$\phi(x) = \frac{\phi_0 x}{\Lambda_x} \Rightarrow \boxed{e^{i\phi(x)} = \sum_{n=-\infty}^{\infty} c_n \, e^{i\frac{2\pi}{\Lambda_x}nx}}$$

- We find the Fourier coefficients as follows:

$$c_n = \frac{1}{\Lambda_x}\int_0^{\Lambda_x} e^{i\frac{\phi_0 x}{\Lambda_x}} e^{-i\frac{2\pi}{\Lambda_x}nx} dx = \frac{1}{\Lambda_x}\int_0^{\Lambda_x} e^{i\frac{2\pi}{\Lambda_x}\left(\frac{\phi_0}{2\pi}-n\right)x} dx$$
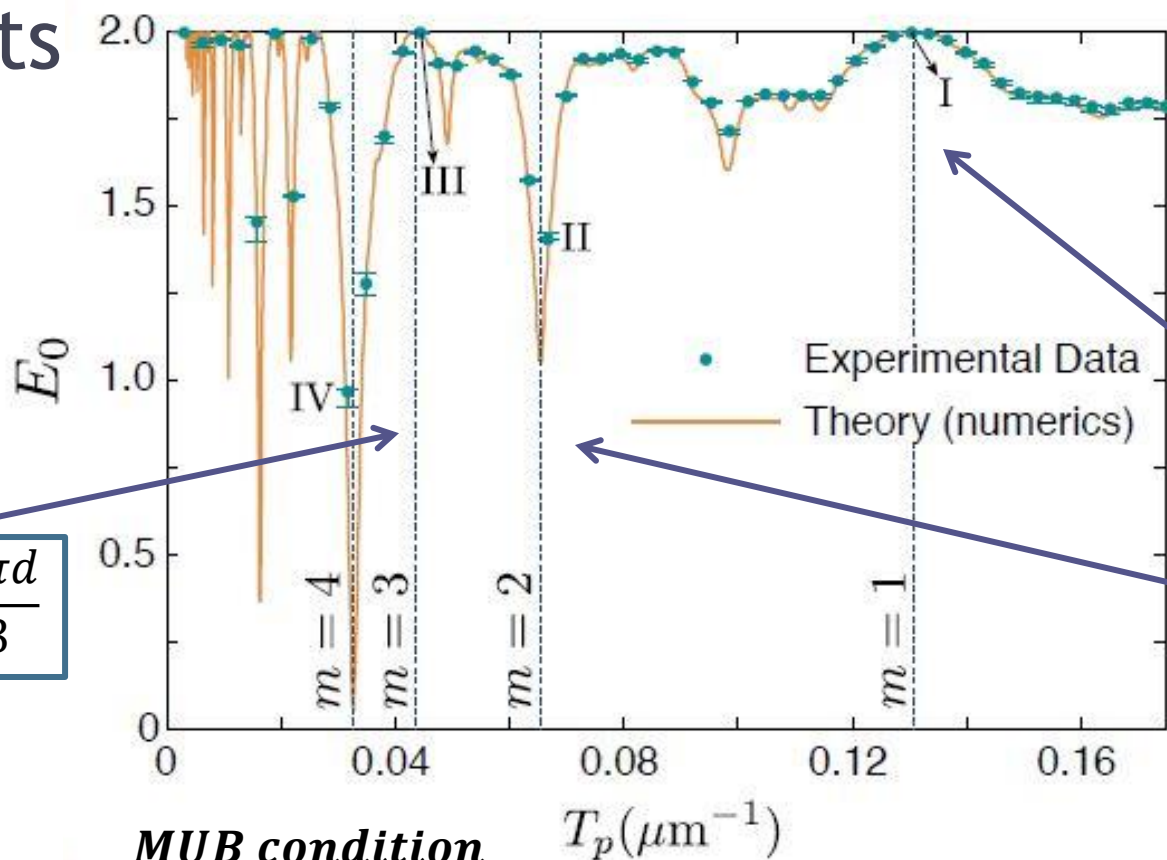
$$c_n = e^{i\pi\left(\frac{\phi_0}{2\pi}-n\right)} sinc\left(\frac{\phi_0}{2\pi}-n\right)$$

- The nth-order diffraction efficiency is:

$$|c_n|^2 = sinc^2\left(\frac{\phi_0}{2\pi}-n\right)$$

> When $\boldsymbol{\phi_0 = 2\pi}$, the **first order** of diffraction becomes the maximum

Results

$T_x T_p = 2\pi d$

$T_x T_p = \dfrac{2\pi d}{3}$

$T_x T_p = \dfrac{2\pi d}{2}$
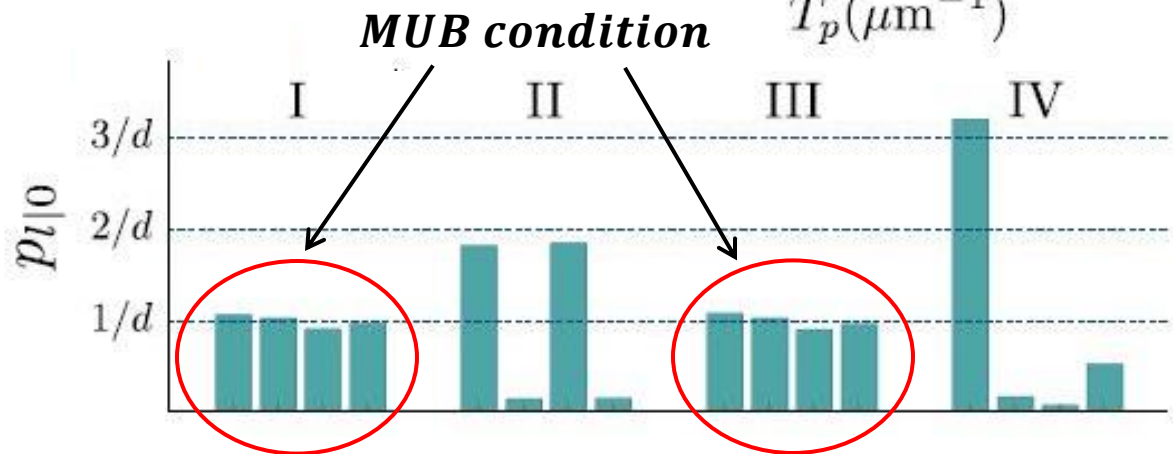
MUB condition

$d = 4$

$T_x = 192 \ \mu m$

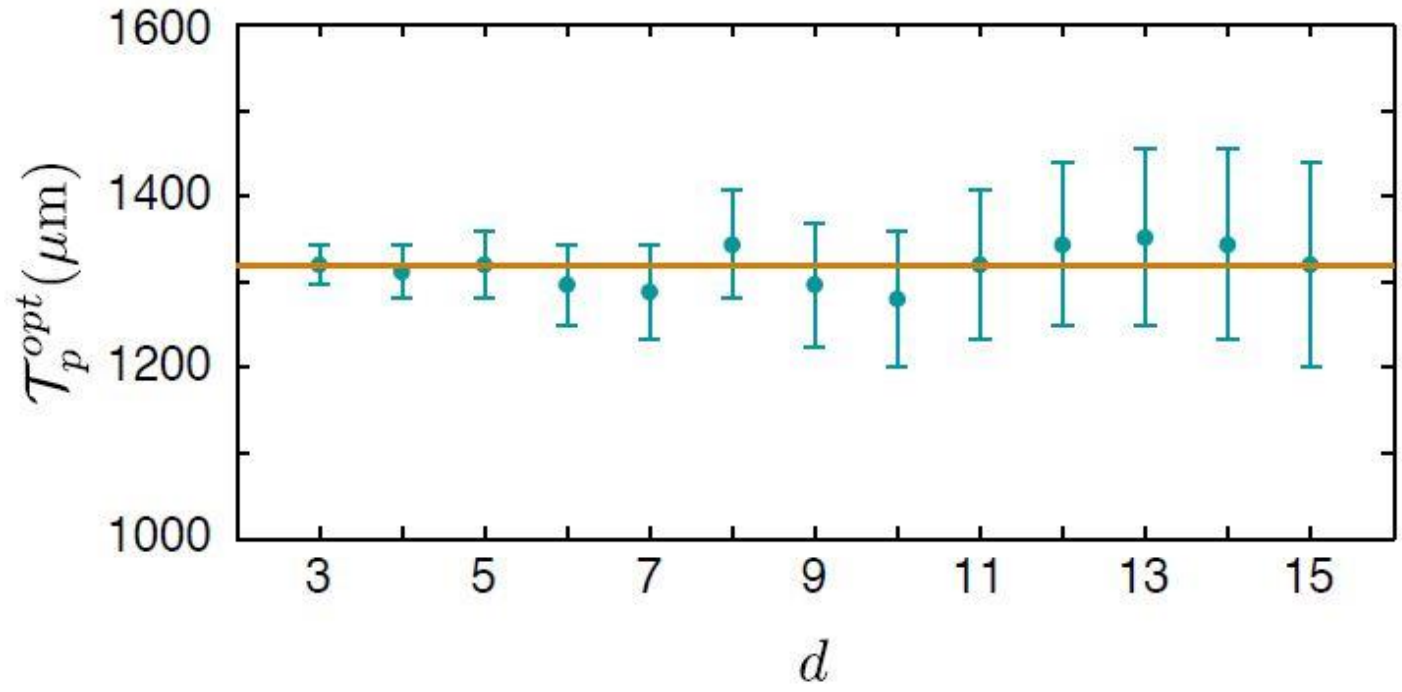$\psi(x) \ \propto \exp(-x^2/2\sigma^2)$

$\sigma = 520 \ \mu m$

Fixed d, variable Tx
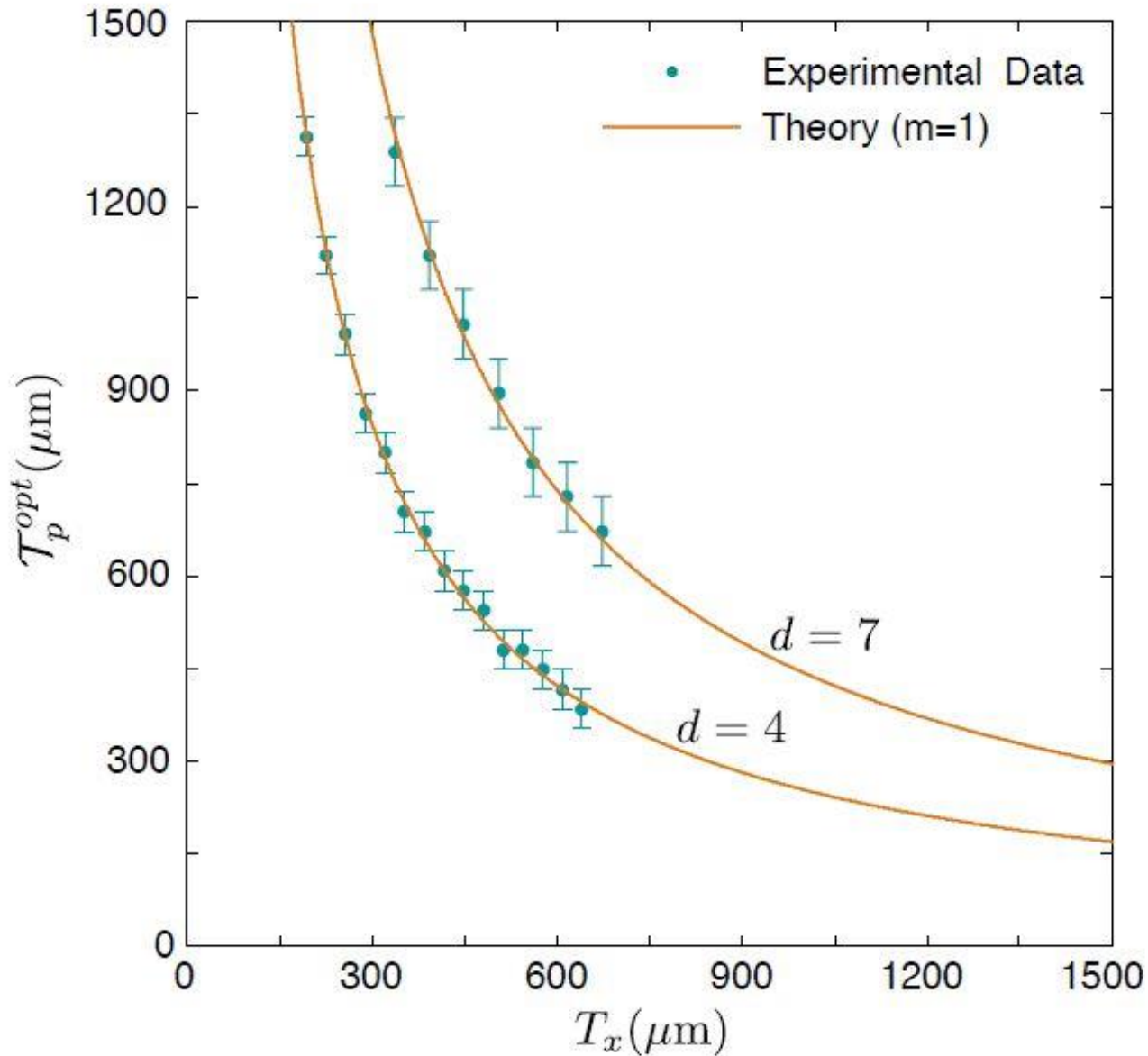
$$\mathcal{T}_p = \frac{f_e \lambda d}{T_x}$$

$$s_p = \frac{f_e \lambda}{s_x d}$$

Fixed Sx, variable d

$$s_p d = \mathcal{T}_p = \frac{f_e \lambda}{s_x}$$

$s_x = 48 \ \mu m$

$\mathcal{T}_p \approx 1319 \ \mu m$

Conclusions

- The MUB condition was verified for different dimensions and periods of PCG masks.

- Our measurements also suggested extra MUB conditions $(m > 1)$ that gave rise to a more complete theoretical description.